研究

Spatially Distributed Beam-Fanning Effect in $BaTiO_3$ Explained with Use of an Asymmetric Gaussian Beam

Jang Doo LEE, Byoung Yoon KIM and Sang Soo LEE

Department of Physics, Korea Advanced Institute of Science and Technology, P. O. Box 150, Chongyang, Seoul, Korea

(Received January 6, 1993; Accepted March 22, 1993)

The beam-fanning effect in a photorefractive $BaTiO_3$ crystal is investigated based on the pattern of the transmitted beam, which is recorded on a photographic plate before generation of phase conjugate waves takes place, and it is explained as the consequence of spatial variation in the refractive index due to photorefractivity and self-phase modulation. The convergent Ar^+ ion laser beam (20 mW) which exhibits a beam-fanning effect in the crystal is approximated by an asymmetric Gaussian beam. The shift of the center of the Gaussian beam increases with increasing incident laser beam diameter. From the equation of the boundary between the beam-fanning region and non-fanning region in the cross section of the transmitted beam, we have obtained n_2 for an extraordinary wave as $(-1.1\pm0.1)\times10^{-11}$ m^2/W at the wavelength of 514.5 nm.

1. Introduction

The beam-fanning effect,[1] often referred to as the asymmetric self-defocusing effect, is the phenomenon wherein coherent light incident on a nonlinear medium is deflected (fanned out) asymmetrically from the incident direction (toward the $+c$ axis of the $BaTiO_3$ crystal in this work). This effect has been observed in $BaTiO_3$,[1] $Sr_{1-x}Ba_xNb_2O_6$(SBN)[2] and $Ba_{2-x}Sr_xK_{1-y}Na_yNb_5O_{15}$ (BSKNN),[3] and is essential to self-pumped phase conjugation.[2-4] This effect was explained by Feinberg[1] as refractive index change proportional to the electric field due to photoelectrons produced by a nonuniform intensity distribution on the tangential plane. Valley[5] also explained the effect as selective amplification of scattered radiation in a near-forward direction due to the photorefractive effect.[6] As an explanation of the spatially distributed beam-fanning effect, Feinberg's model seems more convenient than Valley's model.

In this paper, we report the results obtained from our investigation of the spatial distribution of the beam-fanning effect in the cross section of a converging incident beam. The crystal used is a $BaTiO_3$ single crystal which has the dimensions of $6.5\times6.3\times5.8$ mm^3 space (Sanders Associates, New Hampshire). In the present work, the time dependence of the self-pumped phase conjugation is accurately monitored, and particularly at the beginning of measurements, we found that the beam-fanning effect is separable from the conjugation. In order to explain this effect, we used the approximate intensity distribution of the optical beam in a crystal with an asymmetric Gaussian beam, because a portion of the incident symmetric Gaussian beam fans out asymmetrically in the crystal. As the causes of refractive index change, we consider not only the Pockels effect due to the static electric field that Feinberg calculated, but also the effect of n_2, the nonlinear refractive index coefficient of the crystal for the cw laser beam.[7]

2. Theory

Feinberg calculated the refractive index change due to the photorefractive effect over the cross-sectional area of an incident Gaussian beam with spot size w_0, and attributed the beam-fanning effect to the refractive index change. The relationship is written as $(c/I_0)(\partial/\partial_y)I=-(2cy/w_0^2)\exp\{-(x^2+y^2)/w_0^2\}=(\Delta n)_1$, where n and I are the refractive index and the intensity of the laser beam in the xy plane, respectively. I_0 is the peak intensity of the Gaussian beam and $c=k_BTr_{eff}/2e\pi$,[1] k_B is the Boltzmann constant, T temperature, e the magnitude of charge carriers and r_{eff}

the coefficient of the effective Pockels effect. We note that the differential value due to the Pockels effect on the y-axis (the direction of polarization of the extraordinary ray) alone is induced because of the symmetry of $BaTiO_3$.[1] In addition to $(\Delta n)_1$, we also consider the effect of self-phase modulation as a cause of the refractive index change and represent it as $(\Delta n)_2=n_2I$, where n_2 is the nonlinear refractive index coefficient and I is the laser beam intensity. $(\Delta n)_2$ is the third-order polarization effect which is proportional to E^3, where E is the electric field of light. In the present work, we investigated the beam-fanning effect as the consequence of spatial variation in the refractive indices $(\Delta n)_1$ and $(\Delta n)_2$, produced by photorefractivity and self-phase modulation, respectively.

In **Fig. 1** the induced refractive index change, $\Delta n=(\Delta n)_1+(\Delta n)_2$, due to an asymmetric or center-shifted Gaussian beam on the y axis is shown schematically. This change of Δn is nonuniform over the cross-sectional area, so that the wavefront should become distorted according to the change. In Fig. 1, the region where $\Delta n>0$ has a higher index of refraction than the outer regions, so that a beam-channeling effect arises. By contrast, in the $\Delta n<0$ region, a self-defocusing effect arises.[1] The change of the beam path due to this change ($\Delta n<0$) in the refractive index brings about the beam-fanning effect. The intensity distribution of an incident beam changes due to the beam-fanning effect, so that the incident beam profile changes from the typical TEM_{00} mode. In the case of a small medial volume, as in the case of the present experiment, the intensity distribution

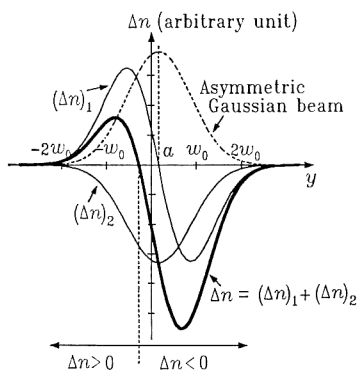

Fig. 1 Schematics of the refractive index change, Δn, approximated by asymmetric Gaussian beam by photorefractivity and self-phase modulation. $(\Delta n)_1=(c/I_0)(\partial/\partial y)I$, $(\Delta n)_2=n_2I$, I: intensity of laser beam, a: shift of the Gaussian beam center.

of a beam within the crystal can be approximated by an asymmetric Gaussian beam. Therefore, the modified intensity distribution having a Gaussian beam-center shift of a is represented, using reduced coordinates $x/w_0=\xi$, $y/w_0=\eta$ and $\alpha=a/w_0$, as

$$I(\xi,\eta,\alpha)=I_0\exp\{-(\sqrt{\xi^2+\eta^2}-\alpha)^2\}. \quad (1)$$

The total change of refractive index caused by this modified intensity distribution is then given by

$$\Delta n=\frac{c}{I_0w_0}\frac{\partial I}{\partial\eta}+n_2I$$
$$=\left\{\frac{-2c}{w_0}(\sqrt{\xi^2+\eta^2}-\alpha)\frac{\eta}{\sqrt{\xi^2+\eta^2}}+n_2I_0\right\}\exp$$
$$\cdot\{-(\sqrt{\xi_2+\eta^2}-\alpha)^2\}. \quad (2)$$

In Eq. (2), the boundary between the focusing and defocusing regions satisfies the condition of zero refractive index change ($\Delta n=0$), namely,

$$-2\pi cw_0\eta\left\{1-\frac{\alpha}{\sqrt{\xi_2+\eta^2}}\right\}+n_2P_0=0, \quad (3)$$

where $P_0(=\pi w_0^2I_0)$ is the total incident power. The ray incident to this boundary is transmitted without any deflection. α and n_2 may be determined from Eq. (3) using the two sets of coordinates, (ξ_1,η_1) and (ξ_2,η_2), taken at the boundary; namely,

$$\alpha=\sqrt{\xi_1^2+\eta_1^2}\left\{1-\frac{\eta_2}{\eta_1\sqrt{\xi_2^2+\eta_2^2}-\eta_2\sqrt{\xi_1^2+\eta_1^2}}\right.$$
$$\left.\cdot(\sqrt{\xi_2^2+\eta_2^2}-\sqrt{\xi_1^2+\eta_1^2})\right\}, \quad (4)$$

$$n_2=\frac{2\pi cw_0}{P_0}\frac{\eta_1\eta_2}{\eta_1\sqrt{\xi_2^2+\eta_2^2}-\eta_2\sqrt{\xi_1^2+\eta_1^2}}$$
$$\cdot(\sqrt{\xi_2^2+\eta_2^2}-\sqrt{\xi_1^2+\eta_1^2}). \quad (5)$$

Equation (3) is represented using x,y coordinates as follows:

$$-2\pi cy+2\pi cw_0\alpha y/\sqrt{x^2+y^2}+n_2P_0=0. \quad (6)$$

In this equation the second term becomes smaller than the other two terms because w_0 becomes smaller as the crystal approaches the focal point of the lens L_3. For $c\simeq10^{-10}$, $w_0\simeq10^{-4}$ (at the neighborhood of the focus), $\alpha\simeq10^{-1}$ and $n_2\simeq10^{-11}$ (see Fig. 6), the second term is on the order of 10^{-15}, whereas the first and third terms are on the order of 10^{-14}. Hence, by ignoring the second term, we obtain

$$y\approx n_2P_0/2\pi c \quad (7)$$

as the solution of the boundary between the beam-fanning and non-fanning regions in the transmitted beam.

Let us now estimate the deflection angle from the differential equations of the light rays in the

medium with a refractive index change. The vector form of the differential equations[8] of the light rays is

$$\frac{\mathrm{d}}{\mathrm{d}s}\left(n\frac{\mathrm{d}\vec{r}}{\mathrm{d}s}\right)=\nabla n, \qquad (8)$$

where $\vec{r}$ is a position vector of a point on a ray, s the optical path length of the ray measured from a fixed point on it, $n=n_0+\Delta n$, and n_0 is the linear index of refraction of the crystal. Since for the linear index of refraction, $(\mathrm{d}/\mathrm{d}s)\{n_0(\mathrm{d}\vec{r}/\mathrm{d}s)\}=\nabla n_0=0$, and $(\mathrm{d}\vec{r}/\mathrm{d}s)$ is the tangential unit vector, $\hat{s}$, along the ray direction, Eq. (8) becomes

$$\frac{\mathrm{d}}{\mathrm{d}s}\{(\Delta n)\hat{s}\}=\nabla(\Delta n). \qquad (9)$$

The y component of Eq. (9) is given by

$$\frac{\mathrm{d}}{\mathrm{d}s}\{(\Delta n)s_y\}=\frac{\partial}{\partial y}(\Delta n). \qquad (10)$$

Through integration, we obtain

$$(\nabla n)s_y=\int\left\{\frac{\partial}{\partial y}(\Delta n)\right\}\mathrm{d}s\approx\left\{\frac{\partial}{\partial y}(\Delta n)\right\}\int\mathrm{d}s\approx\left\{\frac{\partial}{\partial y}(\Delta n)\right\}l_0, \qquad (11)$$

and $s_y=\sin\theta$ (Fig. 4), θ is the beam deflection angle, and $l_0(\simeq 10^{-3})$ is the crystal length, where $\{(\partial/\partial_y)(\Delta n)\}$ is approximated to be constant throughout the ray path in the crystal. From Eq. (2), $\Delta n=(2c\alpha/w_0+n_2I_0)\exp(-\alpha^2)$, $(\partial/\partial y)\Delta n=(1/w_0)(\partial/\partial n)\Delta n=(-2c/w_0^2+2\alpha n_2I_0/w_0)\exp(-\alpha^2)$ for the center ray passing through the point $\xi=0$, $\eta=0$ and $w_0\simeq 10^{-3}$, and α and n_2, which are determined in Section 4, are, respectively, on the order of 10^{-1} and 10^{-11}. Therefore,

$$\sin\theta(\approx\theta)\approx l_0\times\frac{(\partial/\partial y)\Delta n}{\Delta n}$$
$$=l_0\times\frac{-2c/w_0^2+2\alpha n_2I_0/w_0}{2c\alpha/w_0+n_2I_0}, \qquad (12)$$

where $-2c/w_0^2\simeq 10^{-4}$, $2\alpha n_2I_0/w_0\simeq 10^{-5}$, $2c\alpha/w_0\simeq 10^{-8}$ and $n_2I_0\simeq 10^{-7}$. Thus we have $\theta\approx(-2c/w_0^2)/(n_2I_0)\simeq 10^0$ rad (57°), which indicates that the ray deflection is considerably severe. It is measured, as described in Section 4, by taking a photograph from the side of the crystal.

3. Experimental Procedures

The experimental arrangement is shown in **Fig. 2.** The Ar^+ ion laser beam ($\lambda=514.5$ nm, 20 mW) is polarized to be an extraordinary wave to the crystal by using the Glan-Thomson polarizer P_1. Lens L_1, a microscope objective with magnification $\times 40$, and a pinhole Ph (diameter 40 μm) are used for spatial filtering. By means of lens L_2 with the focal length 3 cm, the laser beam is collimated and then focused by lens L_3 with the focal length 12 cm. The spot size (w_0) of the incident beam is defined as the $1/e$ intensity point of the Gaussian beam, and is determined from the size (radius; $r_0=\sqrt{2}w_0$) of the iris aperture (A_1 in Fig. 2) which allows 87% of the Gaussian beam power to pass through. The c-axis of the crystal is parallel to the 6.5 mm edge. The laser beam is incident at an angle of 55° to the 6.5 mm × 6.3 mm plane. The beam transmitted through the crystal is divided by the beam-splitter Bs_2, and the beam cross section is observed on

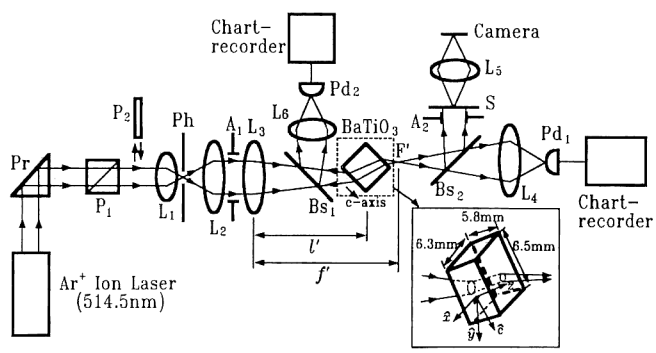

Fig. 2 Experimental setup. The inset shows the dimensions of the crystal and the coordinate system. The z axis is taken to be the direction of propagation of the incident beam. The y axis is chosen to lie in the plane defined by the c axis of the crystal and z axis. Pr: prism, P_1: polarizer, P_2: $\lambda/2$ plate used in erasing process, A_1 and A_2: iris stops, L_1–L_6: lens, Ph: pinhole, Bs_1 and Bs_2: beam splitters, S: screen, Pd_1: photodiode detecting transmitted wave, Pd_2: photodiode detecting phase conjugate wave, F′: focal point of L_3, l': position of the crystal measured from L_3, f': focal length of L_3.

screen S; the power is detected by the photodiode Pd_1. The phase conjugate wave generated by self-pumped phase conjugation is divided by the beam splitter Bs_1, and is detected by photodiode Pd_2.

In order to maintain the same initial conditions in the crystal, an erasing process is applied between measurements, which comprises the following procedures: first, the $\lambda/2$ plate (P_2 in Fig. 2) is used to shift the beam polarization from extraordinary to ordinary polarization, and the crystal is illuminated uniformly for 5 min. This process erases the grating recorded during the previous experiment. After this process, in order to avoid any possible change of the refractive index due to temperature rise caused by laser beam absorption[9] during the previous experiment, the laser beam is blocked and the crystal is left to cool to room temperature for 20 min.

In **Fig. 3,** the powers of the transmitted beam and phase conjugate beam are shown as a function of time. The decrease of the transmitted beam occurs in two steps. The first step takes 25s, as indicated by A and D in Fig. 3. In this short period of time, the beam-fanning effect alone takes place, and the phase conjugate beam is not yet generated. The phase conjugate beam is generated in the second step which begins from point D, where $t=25$ s. Therefore, in order to investigate the beam-fanning effect seperately from the self-pumped phase cojugation effect, we must take data only in the first transient steady state which lasts for 20 s. ($\overline{BD}$ in Fig. 3)

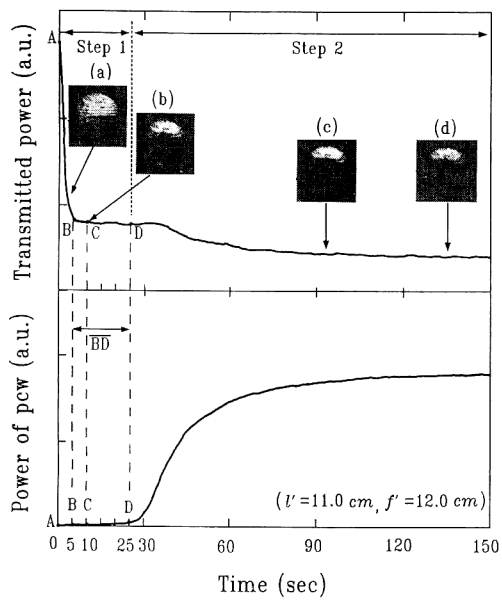

Fig. 3 Time dependence of the cross-sectional pattern, the integrated power of the transmitted wave and the phase conjugate signal. Experimental data are taken at time t, $5s<t<25s$, or $\overline{BD}$ on the time axis. The distance from the lens L_3 to the crystal is 11.0 cm.

4. Experimental Results and Discussion

Figure 4 shows a photograph of the yz plane of the transmitting laser beam in the crystal. This shows that the incident beam is divided into two parts, a transmitted and a fanned part. The beam is deflected by 50.5° from the incident direction, as seen in Fig. 4. This result agrees approximately with the theoretical estimation made using Eq. (12).

Figure 5(a) shows a photograph of the cross section (xy plane) of the transmitted beam observed on the screen, S in Fig. 2, when the crystal is placed at $l'=10.5$ cm. It indicates that the lower part of the incident beam is depleted by the beam-fanning effect. Figure 5(b) illustrates the theoretical profile of the transmitted beam. In this figure, the boundary between the two regions obtained using Eq. (3) and the two data points A ($\xi=0$, $\eta=-0.51$) and B ($\xi=0.97$, $\eta=-0.14$), taken from the transmitted beam pattern, are shown. The shift of the Gaussian beam α is 0.43 and the nonlinear refractive index coefficient n_2 is $-1.1\times10^{-11}(m^2/W)$. Here we approximated T as room temperature (300K) and we also used the numerical value 1.0×10^{-7} of r_{eff}, which was obtained by Feinberg[1] with

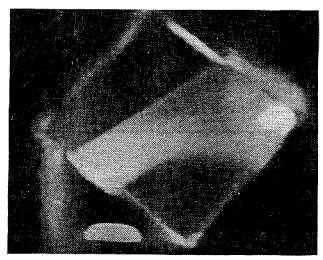
(l'=10.7 cm)

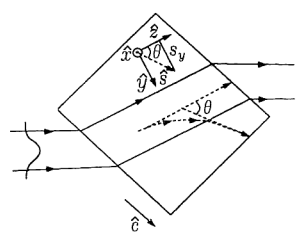

Fig. 4 Photograph of the beam path inside the crystal. θ is the deflection angle.

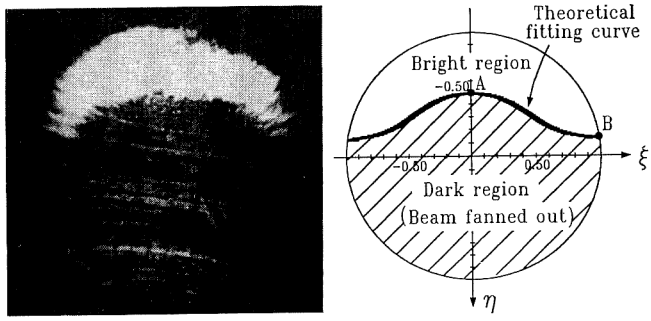

(l'=10.5 cm)　　(n_2=−1.1×10^{-11}, α=0.43)

(a)　　(b)

Fig. 5　(a) Photograph of the cross-sectional pattern of the transmitted wave and (b) theoretically fitted pattern. A=(0.00, −0.51) and B=(0.97, −0.14) are the experimentally obtained points. c=4.2×10^{-10} m^3/W, position of the crystal: l'=10.5 cm.

300 K lattice temperature.

In **Fig. 6** we observe the variation of the pattern of the transmitted beam as a function of incident beam size w_0 or position l' varied by moving lens L_3 in Fig. 2. The four numerical values of α and n_2 listed in this figure were determined using Eq. (4) and Eq. (5). The points A and B lie on the boundary in each photograph as seen in Fig. 5(b). It is seen that the beam-fanning region becomes larger and at the same time, the shift of the Gaussian beam, α, becomes larger with increasing spot size w_0 of the incident beam. As the position of the crystal approaches the focal point (No. (1) in Fig. 6), nearly half of the incident beam is fanned out. This is attributable to the fact that the boundary equation becomes Eq. (7) as w_0 becomes smaller, which indicates a straight line. From Eq. (7), we obtain $n_2 \approx 2\pi cy/P_0$. Since c and P_0 are positive and the y value of the boundary is negative, we find the sign of n_2 to be negative.

When the center of the crystal is exactly at the focal point of the lens, the beam is inverted

No.	1	2	3	4	5
l' (cm)	11.7	11.0	10.7	10.5	10.3
w_0(mm)	0.25	0.75	1.0	1.1	1.3
Cross-section of the transmitted beam	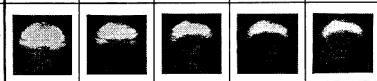				
(ξ,η) of A	—	(0.00,−0.23)	(0.00,−0.39)	(0.00,−0.51)	(0.00,−0.60)
B	—	(0.98,−0.12)	(0.98,−0.13)	(0.97,−0.14)	(0.93,−0.15)
α	—	0.13	0.30	0.43	0.52
n_2 (10^{-11} m^2/W)	—	−1.0	−1.1	−1.1	−1.2

Fig. 6 The patterns of the transmitted wave and α and n_2 values obtained at various positions of the crystal. When l'<10.3 cm, the beam cross section is larger than the crystal.

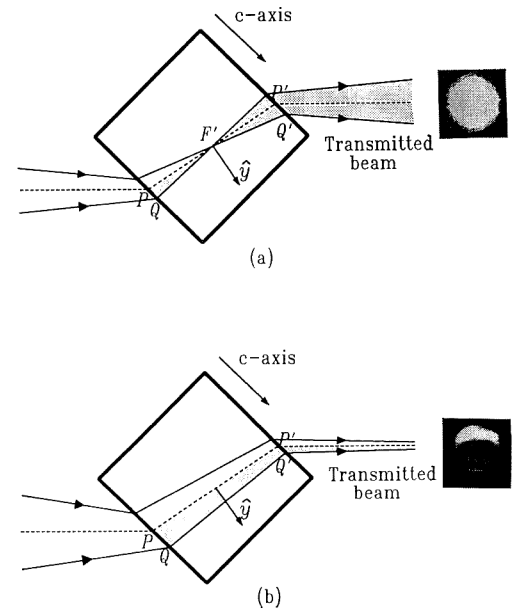

Fig. 7　(a) When the center of the crystal is at the focal point of lens L_3, the beam is inverted. (b) When the focal point of lens L_3 is outside the crystal, beam inversion does not occur. In the shaded area, beam-fanning takes place. The photographs show the transmitted wave pattern for each case.

in the medium, as shown in **Fig. 7**(a); thus the fanning region differs before and after the beam passes through the focal point. Since the fanning lengths of each region become shorter ($\overline{PF'}=\overline{F'P'}\simeq 3$ mm, which is half of the fanning length ($\overline{PP'}$) of case (b) in Fig. 7), the incident beam is far less fanned out. Therefore, the cross section of the transmitted beam has uniform low-level brightness, as shown in the photograph in Fig. 7(a).

5. Conclusions

We have explained the beam-fanning effect as the consequence of nonlinear refractive index changes caused by photorefractivity and self-phase modulation. By approximating the profile of a beam passing inside the crystal as an asymmetric Gaussian beam, and from the spatial intensity distribution in the cross section of the transmitted beam, n_2 for extraordinary waves and the sign are determined at 514.5 nm to be $(-1.1\pm 0.1)\times 10^{-11}$ m^2/W. This value is obtained from the photograph of the transmitted beam before the phase conjugate wave is generated. Data taken while the phase conjugate wave is generated should give a less accurate value of n_2. This is why we have taken the data before the self-pumped phase conjugate wave is generated or before the grating for the phase conjugation is formed. Both the coefficient of the effective Pockels effect of the crystal, r_{eff} and c are dependent on the crystal lattice temperature,[10] which, in this work, are taken to be room temperature. This dependence should be further investigated in order to improve the present results.

References

1) J. Feinberg: "Asymmetric self-defocusing of an optical beam from the photorefractive effect," J. Opt. Soc. Am., **72** (1982) 46-51.
2) G. A. Rakuljic, K. Sayano, A. Yariv and R. R. Neurgaonkar: "Self-starting passive phase conjugate mirror with Ce-doped strontium barium niobate," Appl. Phys. Lett., **50** (1987) 10-12.
3) J. Rodriguez, A. Siahmakoun, G. Salamo, M. J. Miller, W. W. Clark III, G. L. Wood, E. J. Sharp and R. R. Neurgaonkar: "BSKNN as a self-pumped phase conjugator," Appl. Opt., **26** (1987) 1732-1736.
4) J. Feinberg: "Self-pumped, continuous wave phase conjugator using internal reflection," Opt. Lett., **7** (1982) 486-488.
5) G. C. Valley: "Competition between forward- and backward-stimulated photorefractive scattering in $BaTiO_3$," J. Opt. Soc. Am., **B4** (1987) 14-19.
6) N. Y. Kukhtarev, V. Markov and S. Odulov: "Transient energy transfer during hologram formation in $LiNbO_3$ in external electric field," Opt. Commun., **23** (1977) 338-343.
7) S. A. Akhmanov, R. V. Khokhlov and A. P. Sukhorukov: *Laser Handbook II* (North-Holland Publishing Co., Amsterdam, 1972) p. 1151.
8) M. Born and E. Wolf: *Principles of Optics*, 6th ed. (Pergamon Press Inc., New York, 1980) p. 121.
9) D. W. Rush, B. M. Dugan and G. L. Burdge: "Temperature-dependent index-of-refraction changes in $BaTiO_3$," Opt. Lett., **16** (1991) 1295-1297.
10) P. Gunter and J.-P. Huignard: *Photorefractive Materials and Their Applications I* (Topics in Applied Physics, Volume 61, 1988) p. 200.